Bulletin of the Seismological Society of America, Vol. 99, No. 4, pp. 2572–2581, August 2009, doi: 10.1785/0120080340

Short Note

Dependency of Near-Field Ground Motions on the Structural Maturity of the Ruptured Faults

by M. Radiguet, F. Cotton, I. Manighetti, M. Campillo, and J. Douglas

Abstract Little work has been undertaken to examine the role of specific long-term fault properties on earthquake ground motions. Here, we empirically examine the influence of the structural maturity of faults on the strong ground motions generated by the rupture of these faults, and we compare the influence of fault maturity to that of other source properties (slip mode, and blind versus surface rupturing). We analyze the near-field ground motions recorded at rock sites for 28 large (M_w 5.6–7.8) crustal earthquakes of various slip modes. The structural maturity of the faults broken by those earthquakes is classified into three classes (mature, intermediate, and immature) based on the combined knowledge of the age, slip rate, cumulative slip, and length of the faults. We compare the recorded ground motions to the empirical prediction equation of Boore *et al.* (1997). At all frequencies, earthquakes on immature faults produce ground motions 1.5 times larger than those generated by earthquakes on mature faults. The fault maturity appears to be associated with larger differences in ground-motion amplitude than the style of faulting (factor of 1.35 between reverse and strike-slip earthquakes) and the surface rupture occurrence (factor of 1.2 between blind and surface-rupturing earthquakes). However, the slip mode and the fault maturity are dependent parameters, and we suggest that the effect of slip mode may only be apparent, actually resulting from the maturity control. We conclude that the structural maturity of faults is an important parameter that should be considered in seismic hazard assessment.

Online Material: List of ground-motion records.

Introduction

The level and variability in earthquake ground motions depend on three main factors: the earthquake source properties, the details of the wave propagation through the heterogeneous transmission medium, and the local site effects (e.g., Douglas, 2003; Mai, 2009). While many studies have been conducted in the last couple of decades to quantify the role of local site effects and to improve our understanding of wave propagation, little work has been done to examine which source properties, other than the earthquake size, may have a strong effect on the ground motions. The only additional source properties that have so far been included in ground-motion studies are the earthquake slip mode (normal, reverse, or strike slip; e.g., Bommer *et al.*, 2003), the regional tectonic setting (e.g., Spudich *et al.*, 1999), and the presence or lack of significant coseismic slip at surface (e.g., Somerville, 2003; Kagawa *et al.*, 2004). On the other hand, several studies have suggested that some of the earthquake source properties strongly depend on some of the intrinsic properties of the long-term faults on which the earthquakes occur. The plate tectonic context (intraplate versus interplate faults; e.g., Scholz *et al.*, 1986), the long-term slip rate (e.g., Anderson *et al.*, 1996), the geometry (e.g., Stirling *et al.*, 1996), and the structural maturity of the long-term faults (Manighetti *et al.*, 2007) have all been recognized as major fault properties having a significant effect on earthquake variability (i.e., variability in stress drop, slip amplitude, rupture length, and magnitude). Because structural maturity depends together on the age, slip rate, cumulative slip, and length of the faults (Manighetti *et al.*, 2007), and hence is an integrated property, it may be the fault property to have the largest impact on the earthquake source. Our specific objective is to examine whether the fault structural maturity has an influence on the near-field ground-motion variability. If such an influence is demonstrated, it may allow significant improvement of the available ground-motion prediction equations (GMPEs), (e.g., Douglas, 2003) mainly by

permitting a better discrimination of the factors responsible for the variability of ground motions between earthquakes.

We analyze near-field ground motions recorded at rock sites for 28 large (M_w 5.6–7.8) shallow crustal earthquakes of various slip modes. Meanwhile, we examine the structural maturity of the long-term faults broken by the analyzed earthquakes. Following Manighetti *et al.* (2007), we assign the faults three different degrees of structural maturity (mature, intermediate, and immature), defined from the combined knowledge of the age, slip rate, cumulative slip, and length of the long-term faults. We then analyze the ground motions as a function of the fault structural maturity but also as a function of the earthquake slip mode and of the existence or absence of coseismic slip at surface. The ground-motion variations are discussed with respect to the empirical prediction equations of Boore *et al.* (1997) as these equations were derived for crustal earthquakes in the same range of magnitude as the events that we analyze. Choice of a different GMPE should not have a significant impact on the conclusions drawn.

Data

A large quantity of high quality near-field seismological records of strong earthquakes is now available (e.g., the Consortium of Organizations for Strong Motion Observation Systems [COSMOS] database, for access information see the Data and Resources section), making it possible to analyze the ground-motion variability in great detail. We found 28 crustal earthquakes for which near-field seismological records are available (Table 1). Those earthquakes are all shallow (i.e., having broken the first 20 km of the crust), so that the depth dependency of the ground motions may be ignored. Consequently, we do not include any subduction event in our analysis. The 28 selected earthquakes span a magnitude M_w between 5.6 and 7.8 and have various slip modes (13 reverse, 12 strike-slip, and 3 normal mechanisms). We do not consider the moderate magnitude earthquakes ($M_w < 6.5$) in our study of surface rupture occurrence because the lack of surface slip for these earthquakes might be a size effect only. Among the 16 earthquakes of magnitude larger than 6.5, 10 earthquakes have clearly broken the surface and 6 are blind rupture earthquakes. To limit the impact of possible local site effects on the ground-motion variability, we only consider records from rock and stiff soil sites from stations less than 80 km away from the earthquake source (to reduce the effect of possible differences in attenuation, as discussed in Boore *et al.* [1997]). Our total database contains 375 horizontal strong-motion records (Ⓔ Table E1 in the electronic edition of *BSSA*). The source-station distance distribution as a function of magnitude is shown in Figure 1. Note that most of the studied earthquakes occurred in the western United States, so that the results of this study may preferentially apply for tectonic settings similar to this region.

Then, following the approach proposed by Manighetti *et al.* (2007), we have examined the structural maturity of the long-term faults ruptured by the 28 selected earthquakes. In the regions where the earthquakes occurred, the long-term active faults are generally well known with the geometry of their surface trace (total length, major segmentation, strike variations, and associated secondary fault networks), initiation age, maximum long-term slip rate, and total cumulative displacements generally already determined. We have thus gathered from the literature all information documenting the total length, initiation age, maximum cumulative displacement, and maximum slip rate on the long-term faults under analysis and used these four long-term parameters (when available) to qualify the structural maturity of the faults (Table 1). This caused us to classify the broken faults into the three classes proposed by Manighetti *et al.* (2007): immature, intermediate, and mature. Details on the way those three classes are defined are given in a footnote of Table 1. We end up with our fault population including 64% of immature faults, 21% of intermediate-maturity faults, and 15% of mature faults. While defining the maturity of the faults, we note that because they are young, thus small and not generally having a clear surface expression, the immature faults are often less documented than the mature and intermediate faults (Table 1). In the absence of other clear evidence, we consider that a fault that was unknown before an earthquake is an immature fault. All in all, the immature faults, which basically are young and/or slow-slipping faults, form a population that markedly differs from the long-established and generally well-known intermediate and mature faults. At some points of our study, this will make us analyze the intermediate and mature faults together, in order to the clearly different the population of immature faults.

Analysis

We determine the pseudoacceleration response spectra of the ground motions in the period range 0.1–2 sec and compare them to the empirical ground-motion predictions previously proposed by Boore *et al.* (1997) for nonspecified style of faulting. The model of Boore *et al.* (1997) predicts response spectral pseudoacceleration as a function of moment magnitude, distance, and site condition. We selected this equation as a reference because it was derived from shallow crustal earthquakes in the same range of magnitude (M_w 5.3–7.7) as the events of our database (M_w 5.6–7.8), and it additionally allows the specification of the site conditions. We set the shear-wave velocity averaged over the upper 30 m of the ground (V_{S30}) to 620 m/sec as suggested by Boore *et al.* (1997) for generic rock sites.

For each period and station, we determine the residual as the difference between the common logarithm of the response spectra of recorded horizontal motion and the logarithm of the horizontal acceleration predicted using the GMPEs of Boore *et al.* (1997). Figure 2 shows the separate data analysis for earthquakes having occurred on immature (Fig. 2a–c), intermediate-maturity (Fig. 2d), and mature (Fig. 2e) faults. Each line on the plots in Figure 2 represents

Table 1

Structural Maturity of the Long-Term Faults Broken by the Analyzed Earthquakes and Characteristics of the Earthquakes

Number	Date (dd/mm/yyyy)	Earthquake Name	Country	M_w	Style of Faulting	Style of Rupture	Fault Name	L^* (km)	I-Age† (m.y.)	D_{total}‡ (km)	MR§ (cm/yr)	Maturity‖	References#
1	09/02/1971	San Fernando	USA	6.6	reverse	surface	Transverse Ranges fault zone: San Fernando fault	< 200	6		~0.5	1	31, 43, 18
2	01/08/1975	Oroville	USA	6	normal	—	Sierra Nevada fault system: small, secondary fault				< 0.1	1	31
3	13/08/1978	Santa Barbara	USA	5.8	reverse	—	fault	~10			0.01	1	31, 46
4	16/09/1978	Tabas	Iran	7.3	reverse	surface	north ending of Nayband fault: Tabas fault	< 100				1	4, 45
5	06/08/1979	Coyote Lake	USA	5.7	strike-slip	—	Calaveras fault	200		24	1.5 ± 0.4	2	18, 36, 41
6	15/12/1979	Imperial Valley	USA	6.5	strike-slip	surface	Imperial Valley fault (south part of San Jacinto fault)	> 300		24	1.5–2	2	18, 19, 31
7	25/05/1980	Mammoth Lake	USA	6.2	normal	—	Hilton Creek fault zone	~20			~0.1	1	1, 5, 14
8	02/05/1983	Coalinga	USA	6.3	reverse	—	Coalinga thrust fault	~110			0.1–0.2	1	40
9	24/04/1984	Morgan Hill	USA	6.1	strike-slip	—	Calaveras fault	200		24	1.5 ± 0.4	2	18, 36, 41
10	23/12/1985	Nahanni	Canada	6.7	reverse	buried	south Mackenzie fold belt: English Chief anticline	~60			< 0.1	1	22, 48
11	08/07/1986	North Palm Spring	USA	6	reverse	—	San Gorgonio fault zone: Banning and Garnet Hill faults	~100			< 0.2	1	18, 30
12	21/07/1986	Chalfant Valley	USA	6.2	strike-slip	—	White Mountain fault zone	~100			0.05–0.12	1	8, 12, 39
13	02/03/1987	Edgecumbe	USA	6.5	normal	surface	Edgecumbe fault (Whakatane graben)	~10			0.1–0.2	1	3, 29
14	01/10/1987	Whittier Narrows	USA	5.9	reverse	—	Transverse Ranges fault zone: Elysian Park thrust		2–4	10	0.17–0.53	1	10, 31
15	18/10/1989	Loma Prieta	USA	6.9	reverse	buried	Sargent fault	< 100			0.3	1	18, 31
16	28/06/1991	Sierra Madre	USA	5.6	reverse	—	Transverse Range region, Sierra Madre fault zone, Clamshell–Sawpit faults	15–20			< 0.1	1	15, 17, 19
17	19/10/1991	Uttarkashi	India	6.8	reverse	buried	Main Central thrust zone	> 1000				3	9, 24
18	13/02/1992	Erzincan	Turkey	6.6	strike-slip	surface	central section of North Anatolian fault	1000–1500	11–13	~100	1.5–3	3	20, 35, 47
19	28/06/1992	Landers	USA	7.3	strike-slip	surface	eastern California shear zone: Johnson Valley–Emerson–Camprock fault system	< 200			0.05–0.1	1	18, 19, 31, 32, 33

(*continued*)

Table 1 (*Continued*)

Number	Date (dd/mm/yyyy)	Earthquake Name	Country	M_w	Style of Faulting	Style of Rupture	Fault Name	L^* (km)	I-Age† (m.y.)	D_{total}‡ (km)	MR§ (cm/yr)	Maturity‖	References#
20	17/01/1994	Northridge	USA	6.6	reverse	buried	Transverse Ranges fault zone : Northridge fault (eastern extension of Oak Ridge fault)	< 100	2.3–0.5		0.1–0.5	1	11, 15, 18, 19, 21, 43
21	16/01/1995	Kobe**	Japan	6.9	strike-slip		Nojima fault	~10	< 5		0.05–0.1	1	6, 28
22	17/08/1999	Izmit	Turkey	7.6	strike-slip	surface	western tip of North Anatolian fault	1000–1500	~5	85	~1.5	2	2, 20, 42
23	20/09/1999	Chi-Chi	Taiwan	7.6	reverse	surface	Chelungpu fault	100–200	0.7	~14	1.3 ± 0.5	2	7, 38, 49
24	16/10/1999	Hector Mine	USA	7.1	strike-slip	surface	eastern California shear zone: Lavis Lake fault, Bullion fault	< 200			0.05–0.1	1	18, 19, 32, 33, 34
25	12/11/1999	Duzce	Turkey	7.1	strike-slip	surface	western tip of North Anatolian fault	1000–1500	~5	85	~1.5	2	2, 20, 42
26	03/11/2002	Denali	USA	7.8	strike-slip	surface	Denali fault system	~2000	> 30	~130	0.9–1.3	3	13, 25, 27
27	22/12/2003	San Simeon	USA	6.6	reverse	buried	Oceanic fault or adjacent blind thrust	< 100			< 0.1	1	16, 23, 26
28	28/09/2004	Parkfield	USA	6	strike-slip	—	San Andreas fault	> 1000		> 150	~3	3	37, 41, 18

*L is the long-term fault length.

†I-Age is the age of fault initiation in millions of years (m.y.).

‡D_{total} is the maximum cumulative displacement.

§MR is the maximum long-term slip rate.

‖Numbers in this column define the classes of fault maturity: 1 is immature, 2 is intermediate, and 3 is mature. These three classes of structural maturity are based on the criteria L, I-Age, D_{total}, and MR (see Manighetti *et al.*, 2007 for details). Immature: $L < 300$ km, and/or I-Age < 5 m.y., and/or MR < 1 cm/yr, and/or $D_{total} < 10$ km. Intermediate: $300 < L < 1000$ km, and/or $5 <$ I-Age < 10 m.y., and/or MR ≈ 1 cm/yr, and/or $D_{total} = 10$–100 km. Mature: $L > 1000$ km, and/or I-Age > 10 m.y., and/or MR > 2 cm/yr, and/or $D_{total} > 100$ km. A fault does not need to satisfy all of the previous criteria for its maturity to be defined, as the criteria values depend on the fault slip mode. The slip mode of each earthquake is determined according to the classification proposed by Boore *et al.* (1997). Only earthquakes with $M_w \geq 6.5$ that have not broken the ground surface are considered as blind. Others are labeled surface for surface-breaking earthquakes.

#(1) Archuleta *et al.* (1982); (2) Armijo *et al.* (1999); (3) Beanland *et al.* (1990); (4) Berberian (1979); (5) Berry (1997); (6) Boullier *et al.* (2004); (7) Chen *et al.* (2001); (8) Cockerham and Corbett (1987); (9) Cotton *et al.* (1996); (10) Davis *et al.* (1989); (11) Davis and Namson (1994); (12) dePolo and Ramelli (1987); (13) Doig (1998); (14) Given *et al.* (1982); (15) Griffith and Cook (2005); (16) Hardebeck *et al.* (2004); (17) Hauksson (1994); (18) U.S. Geological Survey (2009); (19) Southern California Earthquake Data Center (2009); (20) Hubert-Ferrari *et al.* (2002); (21) Huftile and Yeats (1996); (22) Hyndman *et al.* (2005); (23) Lettis *et al.* (2004); (24) Yu *et al.* (1995); (25) Matmon *et al.* (2006); (26) McLaren *et al.* (2008); (27) Miller *et al.* (2002); (28) Murata *et al.* (2001); (29) Naim and Beanland (1989); (30) Nicholson (1996); (31) Petersen and Wesnousky (1994); (32) Rockwell *et al.* (2000); (33) Rubin and Sieh (1997); (34) Rymer *et al.* (2002); (35) Sengor *et al.* (2004); (36) Schaff *et al.* (2002); (37) Sieh and Jahns (1984); (38) Simoes *et al.* (2007); (39) Smith and Priestley (2000); (40) Stein and Ekstrom (1992); (41) Stirling *et al.* (1996); (42) Talebian and Jackson (2002); (43) Tsutsumi and Yeats (1999); (45) Walker *et al.* (2003); (46) Wallace *et al.* (1981); (47) Westaway (1994); (48) Wetmiller *et al.* (1988); (49) Yue *et al.* (2005).

**The Kobe earthquake was blind where the strong motions have been measured.

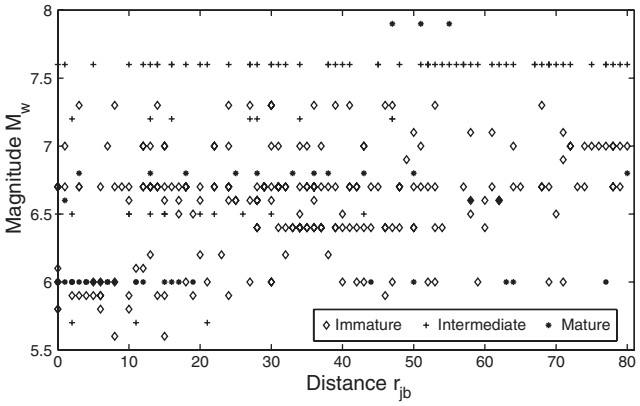

Figure 1. Distribution of recordings in magnitude and distance (r_{jb} is the Joyner and Boore distance). The data are separated into three classes depending on the structural maturity of the faults broken by the analyzed earthquakes.

the residuals for one earthquake averaged over all the recording stations. As a large number of earthquakes have occurred on immature faults, for clarity, we discriminate their ground-motion records as a function of the number of recording stations. Plots in Figure 2a,b that include earthquakes recorded at more than 10 and at 3–10 stations, respectively, are thus the best constrained. The zero line is where there is no bias with respect to the model of Boore *et al.* (1997). Lines above the zero reference indicate earthquakes whose ground motions exceed the model predictions. Note that a 0.1 unit of common logarithm equals a factor of nearly 1.26.

In the period range considered, the ground motions generated by earthquakes on immature faults (best-constrained plots in Fig. 2a,b) generally exceed the model level, while those generated by earthquakes on mature faults (plot in Fig. 2e) are systematically lower than the prediction level. The ground motions produced by earthquakes on immature faults are therefore larger than those generated by earthquakes on mature faults. The earthquake rupturing faults of intermediate maturity (plot in Fig. 2d) have ground motions on both sides of the reference level but most of them (four out of six) have motions below this level.

To compare the influence of fault structural maturity with other source parameters, we then classify the recorded ground motions according to (1) the structural maturity of the long-term ruptured faults; (2) the faulting mechanism of the earthquakes (reverse and strike-slip categories as defined by Boore *et al.* [1997], normal events are too few to be analyzed separately); and (3) the existence or absence of significant surface slip. Because there are few earthquakes on mature faults and because, as discussed before, intermediate and mature faults are in any case far more mature than any immature fault, we analyze together the earthquakes that occurred on intermediate and mature faults in the following. All the parameters eventually assigned to the earthquakes are reported in Table 1.

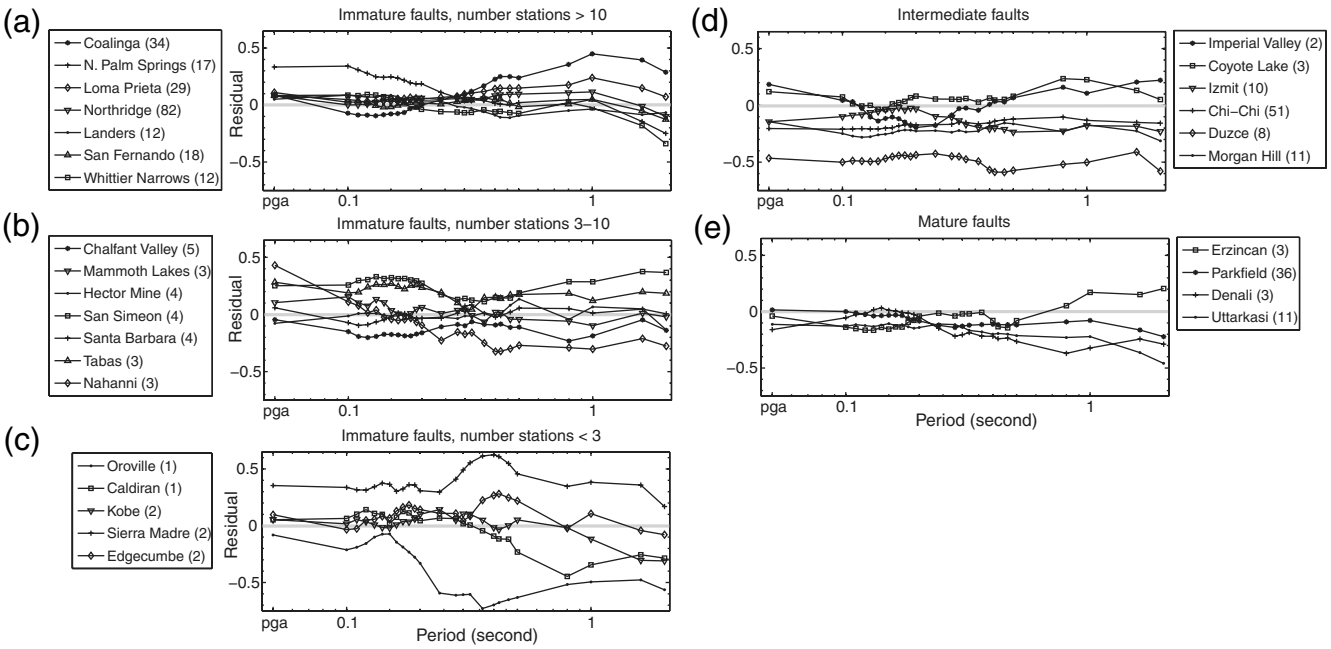

Figure 2. Ratio of response spectral amplitude of individual earthquakes averaged over recording sites to that of the GMPEs of Boore *et al.* (1997). The zero line represents no bias with respect to the GMPE. The residuals represent the common logarithm of the event/model ratio: +0.1 indicates that the average event ground motion exceeds the model by a factor of 1.26 and −0.1 indicates event ground motion at 0.79 of model value. The number of recording stations for each earthquake is indicated in the legend. (a), (b), and (c) show residuals for earthquakes on immature faults; (d) and (e) show earthquakes on intermediate and mature faults, respectively.

To examine how the strong motions vary as a function of the parameters defined previously, we use two different methods. First, following Kagawa *et al.* (2004), we average the residuals for all earthquakes pertaining to any of the categories defined previously. Figure 3a–c shows the averaged residuals as a function of the structural maturity of the broken fault (Fig. 3a), the slip mode of the earthquakes (Fig. 3b), and the existence or lack of significant surface break (Fig. 3c). It confirms that motions produced by the rupturing of immature faults are systematically higher by a factor of 1.35 (0.13 units of common logarithm) than motions generated by earthquakes on mature faults. When earthquakes are distinguished by their mechanism, the same order of difference is observed (factor 1.35), with ruptures on reverse faults producing larger strong motions than earthquakes on strike-slip faults. By contrast, we observe a smaller difference (factor of 1.12) in the ground motions produced by blind and surface-breaking earthquakes.

Then following Spudich *et al.* (1999), we use a more sophisticated method to determine the mean value of the residuals (called the bias) and its standard deviation for each group of earthquakes. This method allows the residuals to be weighted by the number of records. Figure 3d–f confirms the previous observations. As a matter of fact, the ground motions generated by earthquakes on immature faults are systematically higher by a factor of 1.5 (0.18 units of common logarithm) than the ground motions generated by earthquakes on mature faults at all frequencies. The difference in the weighted mean (bias) between the two categories is increased compared to the case where residuals are not weighted (Fig. 3a). The ground-motion difference due to the style of faulting is the same as in Figure 3b (unweighted average) with ground motions on reverse faults that are 1.35 times higher than those on strike-slip faults. The surface rupture occurrence seems to have less influence on the ground motions as blind earthquakes apparently generate ground motions 1.2 times higher than surface-breaking earthquakes for periods lower than 1 sec (the difference is slightly increased compared to Fig. 3c).

When we determine the bias following the Spudich *et al.* (1999) approach (weighted average), a larger difference is observed in the average of residuals on mature versus immature faults, compared to the unweighted study. The ground-motion differences due to the fault maturity are thus larger than those due to the style of faulting. Our results also show that the standard deviations associated with the fault maturity

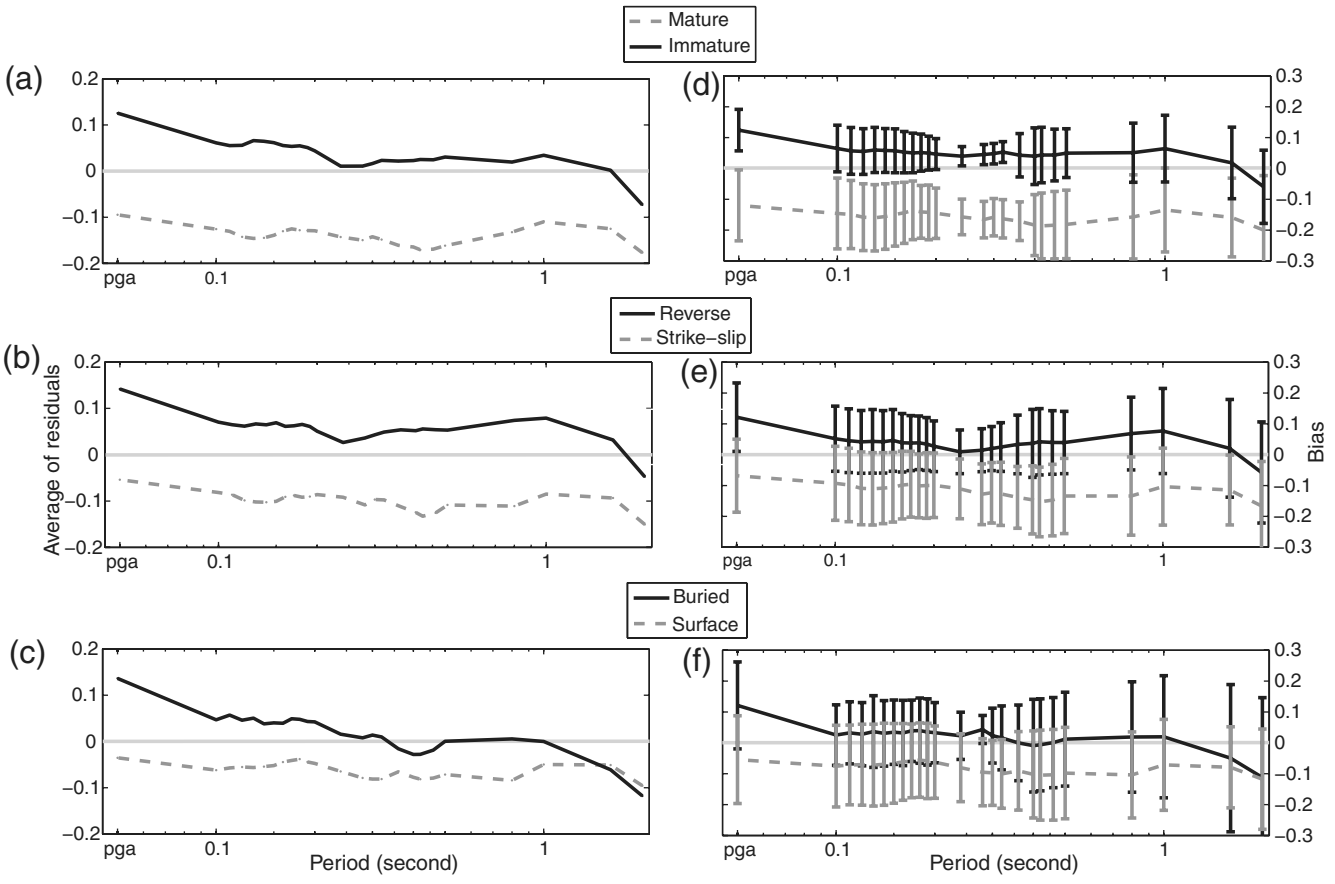

Figure 3. Comparison of the influence of different source factors on the ground motions. (a), (b), and (c) Plots showing the average of residuals (the common logarithm of the event/model ratio) for events following Kagawa *et al.*'s method; (d), (e), and (f) plots show weighted average of residuals and standard deviation following Spudich *et al.*'s method. The source parameters considered are (a) and (d) fault maturity; (b) and (e) style of faulting; (c) and (f) existence or absence of surface break.

classification (Fig. 3d) are lower than the standard deviations associated with the other classifications (style of faulting or surface rupture occurrence), where most error bars overlap.

Our results thus suggest that among the parameters studied, the fault structural maturity is the one to have the most influence on ground motions because it generates the largest differences and the lowest standard deviations. The style of faulting also appears to have a significant effect on ground motions. Yet, it is important to note that there is a dependency between the two factors in our data set as 11 out of 13 of the reverse faults are immature while 8 out of 12 of the strike-slip faults are intermediate or mature. To check whether the effect of fault maturity on ground motions is real or apparent, we test the influence of fault maturity on earthquakes having the same style of faulting. Figure 4a,b shows the averaged residuals computed following Kagawa *et al.* (2004) and Spudich *et al.* (1999), respectively, for strike-slip earthquakes discriminated from the structural maturity of their broken faults. The difference between ground motions on immature and mature faults still appears, though it is smaller than before (averaging a factor of 1.18 for the unweighted average and 1.25 for the bias). Going back to the entire earthquake population, we note that the only two reverse earthquakes that have occurred on mature and intermediate faults (1991 Uttarkashi and 1999 Chi-Chi earthquakes) do not have residuals particularly higher than those of the other earthquakes having broken mature and intermediate faults (Fig. 2d,e). Thus, the low residuals observed for these two earthquakes do not result from the style of faulting only. Together these results make us suggest that the fault structural maturity is likely the parameter accounting for those low residuals.

Our observations thus show that independently of the style of faulting, the fault structural maturity has an influence on the earthquake ground motions. The two parameters are not independent, however, and they both affect the earthquakes ground motions. We suggest that the effect on ground motions commonly attributed to the faulting mechanism is only apparent and more likely results from the fault structural maturity control.

Discussion and Conclusions

Since the 1930s when the first strong-motion networks were installed, the ground-motion records have been used to derive empirical GMPEs that describe how ground motions vary as a function of a limited number of independent parameters, namely the earthquake magnitude, the source-site distance, and some site-specific parameters.

Most of the available equations are summarized and compared in the review article of Douglas (2003). This synthesis highlights that available equations significantly differ from one to the other and that the uncertainties in all equations have not decreased in the last 30 yr. The large uncertainties suggest that some of the factors that govern the ground-motion variability have not been included in the GMPEs.

Reducing both the aleatory and the epistemic uncertainties that affect the ground-motion predictions is thus a key challenge for engineering seismologists. Following Douglas (2003), we suggest that the large intrinsic and epistemic uncertainties partly result from our incomplete understanding of the factors that govern the ground-motion variability and that adding more independent parameters to the GMPEs should reduce the ground-motion variability. In addition to the path and site effects, the few sources parameters (other than the earthquake size) that have been included in the equations are the earthquake mechanism (normal, reverse, or strike-slip; e.g., Bommer *et al.*, 2003), the regional tectonic setting (commonly defined by the earthquakes' geographical location; e.g., Spudich *et al.*, 1999), and the presence or lack of significant coseismic slip at surface (e.g., Somerville, 2003; Kagawa *et al.*, 2004). Recent reviews suggest other parameters that could be included in GMPEs: Douglas (2003) suggests considering the static stress drop and Anderson *et al.* (2000) suggest the total fault offset.

Though the earthquake static stress drop varies in a narrow range, its variation generates large differences in the radiated energy and displacement produced on the rupture plane (for a given length). It is thus likely that stress-drop variations have significant effects on ground-motion variability. Recently, it has been shown that the earthquake static stress drop strongly depends on the structural maturity of

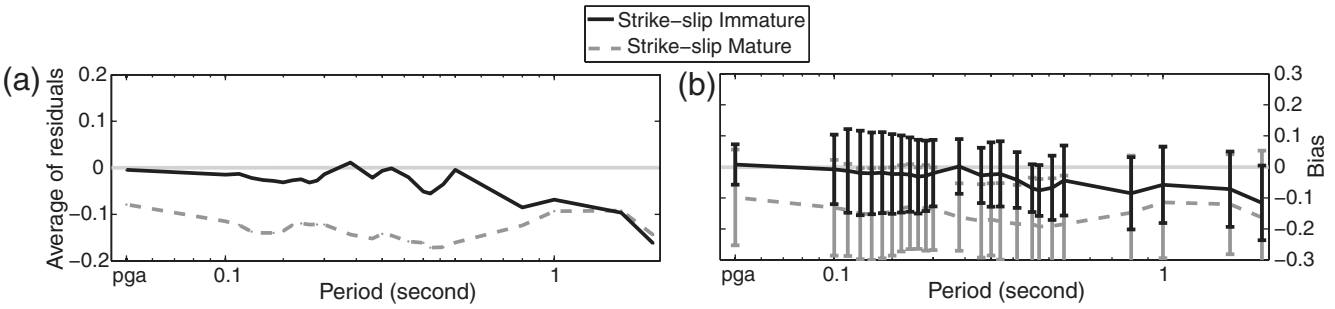

Figure 4. Influence of fault maturity with a constant style of faulting (strike slip). (a) Average of residuals (using the approach of Kagawa *et al.*, 2004). (b) Weighted average of residuals (using the approach of Spudich *et al.*, 1999).

the broken faults (Choy and Kirby, 2004; Manighetti *et al.*, 2007); faults that have been slipping for long and/or slipping at a fast rate obviously break in lower stress-drop earthquakes than young, immature faults (Scholz *et al.*, 1986; Anderson *et al.*, 1996; He *et al.*, 2003). The stress-drop difference would result from the strength and friction on the fault plane reducing as the fault accumulates more slip in time (Ben-Zion and Sammis, 2003; Choy and Kirby, 2004; Choy *et al.*, 2006). Manighetti *et al.* (2007) propose a way through which the structural maturity of the long-term faults can be assessed before those faults break in an earthquake. This offers the possibility of including the fault structural maturity in GMPEs and to use it as an independent parameter that basically describes the expected earthquake static stress drop.

This is what we have done in the present analysis. Using the criteria proposed by Manighetti *et al.* (2007), we have determined the degree of structural maturity of the long-term faults broken by the earthquakes under analysis. We have then used the maturity parameter to classify the ground-motion records and analyze their behavior separately in each of the maturity classes. The results show (Fig. 3a) that, at all frequencies, the ground motions produced by earthquakes having broken immature faults are 1.5 times larger than those generated by earthquakes on mature faults. This suggests that the structural maturity of the long-term faults broken by the earthquakes is an important factor that governs, at least partly, the variability of the near-field strong ground motions. The observed reduction of ground motions with increasing fault maturity is coherent with a lower stress drop for earthquakes on mature faults than on immature faults. These results are also in agreement with the suggestion of Anderson *et al.* (2000) that the low accelerations recorded during the 1999 Izmit and Chi-Chi earthquakes compared to the 1992 Landers and 1994 Northridge earthquakes may be related to characteristics of the broken fault; they suggest that the low accelerations produced are related to smooth fault traces resulting from large geological offsets.

When earthquakes are distinguished by their faulting mechanism (Fig. 3b), we find that ruptures on reverse faults produce ground motions about 1.35 times larger than earthquakes on strike-slip faults. This result is coherent with the range of 1.2–1.4 proposed by Bommer *et al.* (2003) for the ratio of reverse to strike-slip ground motions. The fault maturity thus generates larger difference in the ground motion than the style of faulting. Yet, there is a dependency between the two factors, because most of the mature earthquakes of our data set are strike slip. This may be due to the fact that strike-slip earthquakes are more likely to extend in length and accumulate large offsets than dip-slip earthquakes and, thus, are more likely to become mature faults. When only strike-slip earthquakes are considered (Fig. 4), a difference in the strong-motion amplitude (averaging a factor 1.25) is still observed between earthquakes on immature and mature faults. This suggests that the effect on ground motions commonly attributed to the faulting mechanism may only be apparent and more likely result from the fault maturity control.

Finally, our data show smaller differences in the amplitude of ground motions produced by blind and surface-breaking earthquakes, compared to the results of Somerville (2003) and Kagawa *et al.* (2004), who found that ground motions from buried ruptures are 1.8 times larger than motions produced by surface-breaking earthquakes (in the period range around 1 sec). Our results show, in the same frequency range, that ground motions from buried earthquakes are only 1.25 times (~0.09 units of common logarithm) larger than surface-rupturing earthquakes. Because our results arise from an updated denser dataset that includes only rock and stiff soil sites (contrary to Somerville [2003] and Kagawa *et al.* [2004] studies), we suggest that our data are less likely to be biased by site effects and that they are better constrained than before. This makes us conclude that, for large shallow earthquakes ($M \geq 6.5$), the way the rupture terminates upward has little effect on the ground-motion variability.

We conclude that the degree of structural maturity of the long-term faults is a factor that likely plays a significant role in the strong ground motion variability; when rupturing in large earthquakes, immature faults obviously produce larger ground motions than would mature faults breaking in a similar magnitude earthquake. The structural maturity of a fault can be assessed *a priori* and independently of any knowledge of either the past or future earthquakes. It is thus an independent parameter that should be included in the GMPEs, in addition to the common parameters describing the expected earthquake size, wave propagation path, and site characteristics. One simple way to include the effect of fault structural maturity in the available equations is to apply them with an adjustment factor. Provided that the equation chosen for calculation includes no style of faulting parameter, we suggest that the equation be lowered by a factor of 0.7 when the earthquake is expected to occur on a mature fault and be increased by a factor of 1.12 when the earthquake is expected to occur on an immature fault.

Data and Resources

Accelerograms used in this study are available via the COSMOS online database (http://db.cosmos-eq.org, last accessed May 2009). Ⓔ The list of records used is available in the electronic edition of *BSSA*.

Acknowledgments

The work has been done in the framework of a scientific project (QUAKonSCARPS) funded by the French ANR (Grant Number ANR-06-CATT-008-01). John Douglas's contributions to this study were supported by internal BRGM projects. Fabrice Cotton and Michel Campillo benefited from Institut Universitaire de France support. We thank an anonymous reviewer for useful comments on an earlier version of this article.

References

Anderson, J. G., J. N. Brune, R. Anooshehpoor, and S. D. Ni (2000). New ground motion data and concepts in seismic hazard analysis, *Curr. Sci.* **79,** 1278–1290.

Anderson, J. G., S. G. Wesnousky, and M. W. Stirling (1996). Earthquake size as a function of fault slip rate, *Bull. Seismol. Soc. Am.* **86,** 683–690.

Archuleta, R. J., E. Cranswick, C. Mueller, and P. Spudich (1982). Source parameters of the 1980 Mammoth Lakes, California, earthquake sequence, *J. Geophys. Res.* **87,** 4595–4607.

Armijo, R., B. Meyer, A. Hubert, and A. Barka (1999). Westward propagation of the North Anatolian fault into the northern Aegean: Timing and kinematics, *Geology* **27,** 267–270.

Beanland, S., G. H. Blick, and D. J. Darby (1990). Normal faulting in a back arc basin—geological and geodetic characteristics of the 1987 Edgecumbe earthquake, New Zealand, *J. Geophys. Res.* **95,** 4693–4707.

Ben-Zion, Y., and C. G. Sammis (2003). Characterization of fault zones, *Pure Appl. Geophys.* **160,** 677–715.

Berberian, M. (1979). Earthquake faulting and bedding thrust associated with the Tabas-e-Golshan (Iran) earthquake of September 16, 1978, *Bull. Seismol. Soc. Am.* **69,** 1861–1887.

Berry, M. E. (1997). Geomorphic analysis of late Quaternary faulting on Hilton Creek, Round Valley, and Coyote warp faults, east-central Sierra Nevada, California, USA, *Geomorphology* **20,** 177–195.

Bommer, J. J., J. Douglas, and F. O. Strasser (2003). Style-of-faulting in ground-motion prediction equations, *Bull. Earthq. Eng.* **1,** 171–203.

Boore, D., W. Joyner, and T. Fumal (1997). Site amplifications for generic rock sites, *Bull. Seismol. Soc. Am.* **87,** 327–341.

Boullier, A. M., K. Fujimoto, H. Ito, T. Ohtani, N. Keulen, O. Fabbri, D. Amitrano, M. Dubois, and P. Pezard (2004). Structural evolution of the Nojima fault (Awaji Island, Japan) revisited from the GSJ drill hole at Hirabayashi, *Earth Planets Space* **56,** 1233–1240.

Chen, Y. G., W. S. Chen, J. C. Lee, Y. H. Lee, C. T. Lee, H. C. Chang, and C. H. Lo (2001). Surface rupture of 1999 Chi-Chi earthquake yields insights on active tectonics of central Taiwan, *Bull. Seismol. Soc. Am.* **91,** 977–985.

Choy, G. L., and S. H. Kirby (2004). Apparent stress, fault maturity, and seismic hazard for normal-fault earthquakes at subduction zones, *Geophys. J. Int.* **159,** 991–1012.

Choy, G., A. McGarr, S. H. Kirby, and J. Boatwright (2006). An overview of the global variability in radiated energy and apparent stress, in *Earthquakes: Radiated Energy and the Physics of Faulting*, R. Abercrombie, A. McGarr, and G. Di Toro (Editors), American Geophysical Monograph, **170,** 43–57.

Cockerham, R. S., and E. J. Corbett (1987). The July 1986 Chalfant Valley, California, earthquake sequence—preliminary results, *Bull. Seismol. Soc. Am.* **77,** 280–289.

Cotton, F., M. Campillo, A. Deschamps, and B. K. Rastogi (1996). Rupture history and seismotectonics of the 1991 Uttarkashi, Himalaya earthquake, *Tectonophysics* **258,** 35–51.

Davis, T. L., and J. Namson (1994). A balanced cross-section of the 1994 Northridge earthquake, southern California, *Nature* **372,** 167–169.

Davis, T. L., J. Namson, and R. F. Yerkes (1989). A cross-section of the Los-Angeles area—seismically active fold and thrust belt, the 1987 Whittier-Narrows earthquake, and earthquake hazard, *J. Geophys. Res.* **94,** 9644–9664.

dePolo, C. M., and A. R. Ramelli (1987). Preliminary-report on surface fractures along the White Mountains fault zone associated with the July 1986 Chalfant Valley earthquake sequence, *Bull. Seismol. Soc. Am.* **77,** 290–296.

Doig, R. (1998). Paleoseismological evidence from lake sediments for recent movement on the Denali and other faults, Yukon Territory, Canada, *Tectonophysics* **296,** 363–370.

Douglas, J. (2003). Earthquake ground-motion estimation using strong-motion records: A review of equations for the estimation of peak ground acceleration and response spectral ordinates, *Earth Sci. Rev.* **61,** 43–104.

Given, J. W., T. C. Wallace, and H. Kanamori (1982). Teleseismic analysis of the 1980 Mammoth Lakes earthquake sequence, *Bull. Seismol. Soc. Am.* **72,** 1093–1109.

Griffith, W. A., and M. L. Cooke (2005). How sensitive are fault-slip rates in the Los Angeles basin to tectonic boundary conditions?, *Bull. Seismol. Soc. Am.* **95,** 1263–1275.

Hardebeck, J. L., J. Boatwright, D. Dreger, R. Goel, V. Graizer, K. Hudnut, C. Ji, L. Jones, J. Langbein, J. Lin, E. Roeloffs, R. Simpson, K. Stark, R. Stein, and J. C. Tinsley (2004). Preliminary report on the 22 December 2003, *M* 6.5 San Simeon, California, earthquake, *Seism. Res. Lett.* **75,** 155–172.

Hauksson, E. (1994). The 1991 Sierra-Madre earthquake sequence in southern California—seismological and tectonic analysis, *Bull. Seismol. Soc. Am.* **84,** 1058–1074.

He, C., T.-F. Wong, and N. M. Beeler (2003). Dynamics of a spring-slider system with rate and state dependent friction: Numerical simulations of the effects of loading velocity and recurrence time for two different evolution laws, *J. Geophys. Res.* **108,** no. B1, 2037.

Hubert-Ferrari, A., R. Armijo, G. King, B. Meyer, and A. Barka (2002). Morphology, displacement, and slip rates along the North Anatolian fault, Turkey, *J. Geophys. Res.* **107,** no B10, 2235, doi 10.1029/2001JB000393.

Huftile, G. J., and R. S. Yeats (1996). Deformation rates across the placerita (Northridge M_w 6.7 aftershock zone) and Hopper Canyon segments of the western transverse ranges deformation belt, *Bull. Seismol. Soc. Am.* **86,** S3–S18.

Hyndman, R. D., P. Fluck, S. Mazzotti, T. J. Lewis, J. Ristau, and L. Leonard (2005). Current tectonics of the northern Canadian Cordillera, *Can. J. Earth Sci.* **42,** 1117–1136.

Kagawa, T., K. Irikua, and P. G. Somerville (2004). Differences in ground motion and fault rupture between the surface and buried rupture earthquakes, *Earth Planets Space* **56,** 3–14.

Lettis, W. R., K. L. Hanson, J. R. Unruh, M. McLaren, and W. U. Savage (2004). Quaternary tectonic setting of south-central coastal California, *U.S. Geol. Surv. Bull.* **1995,** no. AA, 21 pp.

Mai, P. M. (2009). Ground motion: Complexity and scaling in the near field of earthquake ruptures, in *Encyclopedia of Complexity and Systems Science*, R. Meyers (Editor), Springer, Berlin (in press).

Manighetti, I., M. Campillo, S. Bouley, and F. Cotton (2007). Earthquake scaling, fault segmentation, and structural maturity, *Earth Planet. Sci. Lett.* **253,** 429–438.

Matmon, A., D. P. Schwartz, P. J. Haeussler, R. Finkel, J. J. Lienkaemper, H. D. Stenner, and T. E. Dawson (2006). Denali fault slip rates and Holocene-late Pleistocene kinematics of central Alaska, *Geology* **34,** 645–648.

McLaren, M. K., J. L. Hardebeck, N. van der Elst, J. R. Unruh, G. W. Bawden, and J. L. Blair (2008). Complex faulting associated with the 22 December 2003 M_w 6.5 San Simeon, California, earthquake, aftershocks, and postseismic surface deformation, *Bull. Seismol. Soc. Am.* **98,** 1659–1680.

Miller, M. L., D. C. Bradley, T. K. Bundtzen, and W. McClelland (2002). Late Cretaceous through Cenozoic strike-slip tectonics of southwestern Alaska, *J. Geol.* **110,** 247–270.

Murata, A., K. Takemura, T. Miyata, and A. Lin (2001). Quaternary vertical offset and average slip rate of the Nojima fault on Awaji island, Japan, *The Island Arc* **10,** 360–367.

Nairn, I. A., and S. Beanland (1989). Geological setting of the 1987 Edgecumbe earthquake, New Zealand, *N. Z. J. Geol. Geophys.* **32,** 1–13.

Nicholson, C. (1996). Seismic behavior of the southern San Andreas fault zone in the northern Coachella valley, California: Comparison of the 1948 and 1986 earthquake sequences, *Bull. Seismol. Soc. Am.* **86,** 1331–1349.

Petersen, M. D., and S. G. Wesnousky (1994). Fault slip rates and earthquake histories for active faults in Southern California, *Bull. Seismol. Soc. Am.* **84,** 1608–1649.

Rockwell, T. K., S. Lindvall, M. Herzberg, D. Murbach, T. Dawson, and G. Berger (2000). Paleoseismology of the Johnson Valley, Kickapoo,

and Homestead Valley faults: Clustering of earthquakes in the eastern California shear zone, *Bull. Seismol. Soc. Am.* **90,** 1200–1236.

Rubin, C. M., and K. Sieh (1997). Loop dormancy, low slip rate, and similar slip-per-event for the Emerson fault, eastern California shear zone, *J. Geophys. Res.* **102,** 15,319–15,333.

Rymer, M. J., G. G. Seitz, K. D. Weaver, A. Orgil, G. Faneros, J. C. Hamilton, and C. Goetz (2002). Geologic and paleoseismic study of the Lavic Lake fault at Lavic Lake playa, Mojave Desert, southern California, *Bull. Seismol. Soc. Am.* **92,** 1577–1591.

Schaff, D. P., G. H. R. Bokelmann, G. C. Beroza, F. Waldhauser, and W. L. Ellsworth (2002). High-resolution image of Calaveras fault seismicity, *J. Geophys. Res.* **107,** no. B9, 2186, doi 10.1029/2001JB000633.

Scholz, C. H., C. Aviles, and S. Wesnousky (1986). Scaling differences between large intraplate and interplate earthquakes, *Bull. Seismol. Soc. Am.* **76,** 65–70.

Sengor, , A. M. C., O. Tuysuz, C. Imren, M. Sakinc, H. Eyidogan, N. Gorur, X. Le Pichon, and C. Rangin (2004). The North Anatolian fault: A new look, *Annu. Rev. Earth Planet. Sci.* **33,** 1–75.

Sieh, K. E., and R. H. Jahns (1984). Holocene activity of the San Andreas fault at Wallace Creek, California, *Geol. Soc. Am. Bull.* **95,** 883–896.

Simoes, M., J. P. Avouac, and Y. G. Chen (2007). Slip rates on the Chelungpu and Chushiang thrust faults inferred from a deformed strath terrace along the Dungpuna river, west central Taiwan, *J. Geophys. Res.* **112,** B03S10, doi 10.1029/2005JB004200.

Smith, K. D., and K. F. Priestley (2000). Faulting in the 1986 Chalfant, California, sequence: Local tectonics and earthquake source parameters, *Bull. Seismol. Soc. Am.* **90,** 813–831.

Somerville, P. G. (2003). Magnitude scaling of the near fault rupture directivity pulse, *Phys. Earth Planet. Interiors* **137,** 201–212.

Southern California Earthquake Data Center (2009). Chronological earthquake index, http://www.data.scec.org/chrono_index/quakedex.html (last accessed May 2009).

Spudich, P., W. B. Joyner, A. G. Lindh, D. M. Boore, B. M. Margaris, and J. B. Fletcher (1999). SEA99: A revised ground motion prediction relation for use in extensional tectonic regimes, *Bull. Seismol. Soc. Am.* **89,** 1156–1170.

Stein, R. S., and G. Ekstrom (1992). Seismicity and geometry of a 110-km-long blind thrust-fault .2. Synthesis of the 1982-1985 California earthquake sequence, *J. Geophys. Res.* **97,** 4865–4883.

Stirling, M. W., S. G. Wesnousky, and K. Shimazaki (1996). Fault trace complexity, cumulative slip, and the shape of the magnitude-frequency distribution for strike-slip faults: A global survey, *Geophys. J. Int.* **124,** 833–868.

Talebian, M., and J. Jackson (2002). Offset on the Main Recent fault of NW Iran and implications for the late Cenozoic tectonics of the Arabia-Eurasia collision zone, *Geophys. J. Int.* **150,** 422–439.

Tsutsumi, H., and R. S. Yeats (1999). Tectonic setting of the 1971 Sylmar and 1994 Northridge earthquakes in the San Fernando Valley, California, *Bull. Seismol. Soc. Am.* **89,** 1232–1249.

U.S. Geological Survey (2009). Cooperator California Geological Survey, http://earthquake.usgs.gov/regional/qfaults/ca/index.php (last accessed May 2009).

Walker, R., J. Jackson, and C. Baker (2003). Surface expression of thrust faulting in eastern Iran: source parameters and surface deformation of the 1978 Tabas and 1968 Ferdows earthquake sequences, *Geophys. J. Int.* **152,** 749–765.

Wallace, T. C., D. V. Helmberger, and J. E. Ebel (1981). A broadband study of the 13 August 1978 Santa-Barbara earthquake, *Bull. Seismol. Soc. Am.* **71,** 1701–1718.

Westaway, R. (1994). Present-day kinematics of the Middle-East and Eastern Mediterranean, *J. Geophys. Res.* **99,** 12,071–12,090.

Wetmiller, R. J., R. B. Horner, H. S. Hasegawa, R. G. North, M. Lamontagne, D. H. Weichert, and S. G. Evans (1988). An analysis of the 1985 Nahanni earthquakes, *Bull. Seismol. Soc. Am.* **78,** 590–616.

Yu, G., K. N. Khattri, J. G. Anderson, J. N. Brune, and Y. Zeng (1995). Strong ground motion from the Uttarkashi, Himalaya, India, earthquake—comparison of observations with synthetics using the composite source model, *Bull. Seismol. Soc. Am.* **85,** 31–50.

Yue, L. F., J. Suppe, and J. H. Hung (2005). Structural geology of a classic thrust belt earthquake: The 1999 Chi-Chi earthquake, Taiwan (M_w 7.6), *J. Struct. Geol.* **27,** 2058–2083.

Laboratoire de Géophysique Interne et Tectonophysique
Centre Nationale de la Recherche Scientifique (CNRS), Observatoire de Grenoble
Université J. Fourier
LGIT, Maison des Géosciences, BP 53
38041 Grenoble Cedex 9, France
(M.R., F.C., I.M., M.C.)

Bureau de recherches géologiques et minières (BRGM)–ARN/RIS
3 avenue C. Guillemin, BP 36009
45060 Orleans Cedex 2, France
(J.D.)

Manuscript received 26 November 2008